Springer

Journal of
Mechanical
Science and
Technology

Journal of Mechanical Science and Technology 22 (2008) 864~870

www.springerlink.com/content/1738-494x

Failure analysis of turbine blade in atomic power plant

Dong Woo Lee[1], Seok Swoo Cho[2], Soon Hyeok Hong[3] and Won Sik Joo[1,*]

[1]*Deptartment of Mechanical Engineering, Dong-A University, 840, Hadan2-dong, Saha-gu, Busan 604-714, Korea*
[2]*Department of Vehicle Engineering, Kangwon National University, 253, Gyo-dong, Samcheok-si, Gangwon-do 245-711, Korea*
[3]*Cooperative Laboratory Center, Pukyong National University, 100, Yongdang-dong, Nam-gu, Busan, 608-739, Korea*

(Manuscript Received July 19, 2007; Revised January 31, 2008; Accepted February 4, 2008)

Abstract

The turbine blade in an atomic power plant may be fractured by fatigue, stress corrosion cracking and bad fitting. Especially, fatigue fracture is caused by low stress amplitude below the yielding stress. SEM fractography does not have striation, but AFM fractography does on the fatigue fractured surface of 12% Cr steel used for the turbine blade. Surface roughness R_q measured by AFM is linearly related to the stress intensity factor range, ΔK, and is increased linearly according to the load range ΔP. Therefore, in this study, the loading condition applied to a turbine blade is predicted by the relation between the intersection of the ΔK-R_q relation and load range ΔP.

Keywords: AFM; Fractography; Plastic zone depth; SEM; Stress intensity factor

1. Introduction

The demand for electric power has increased every year with the increase of living standards and the gradual expansion of production facilities. Accounting for 43% of the domestic electric power production in 1999, atomic power plants have become more and more obsolete every year. At the same time, when one considers that the accidents in atomic power plants have not decreased, it is necessary to take planned preventive maintenance and analyze broken atomic power facilities [1, 2].

Especially, the failure in turbine blades causes an expanded ripple effect of accidents and irregular repairing. Turbine blades may be broken for a variety of reasons including fatigue fracture, corrosion fatigue, stress corrosion, erosion, defective manufacturing and assembling, fault operation, design errors and others, but accidents attributable to fatigue account for the most.

Since the parts fractured by fatigue generate striation at regular intervals, the type of fracture surface and the applied load may be estimated by using a scanning electronic microscope (SEM). However, the striation on the fracture surface may hardly be observed if the material is brittle or the range of crack growth rate is out of the range of fracture analysis. In such case, to investigate the breakage mechanism, Nano-fractography enabling the creation and growth process of fatigue crack in 3-D space with high magnification would be required.

Recently, the scanning tunneling microscope (STM), with which surface was observed in 3-D space at the level of atomic resolution, and the scanning probe microscope (SPM) such as atomic force microscope (AFM) are, therefore, being widely used in various fields.

In the field of material strength evaluation, microscopic deformation mechanisms were investigated by observing the discharge procedure of potential according to plastic deformation around a crack tip [3], and Masuda et al. [4] observed the generation and growth sequence of a corrosion fatigue pit in nm by using STM. Therefore, in order to investigate the cause of failure in a torsion-mounted type turbine

*Corresponding author. Tel.: +82 51 200 7641, Fax.: +82 51 200 7656
E-mail address: wsjoo@dau.ac.kr
DOI 10.1007/s12206-008-0204-4

blade of 12% Cr steel, which is installed and operated in an atomic power plant, this study reviewed the stress intensity factor range and the correlation between interval of striation and surface roughness by atomic force microscope and calculated the load history applied to the turbine blade.

2. Turbine blade failure accidents

The three low-pressure turbine stages use a standard type, torsion-mounted type blade. Table 1 shows the general properties of the three low-pressure turbine stages, which were used for the failure analysis.

Table 1. General properties at third stage of low pressure turbine.

RPM	Steam condition				Number of blade	
	Inlet		Outlet		3 stage	
	operating temp. (℃)	pressure (MPa)	operating temp. (℃)	pressure (MPa)	Rotary wing (EA)	Fixed wing (EA)
1800	252	0.827	33.3	0.0051	143	36×2

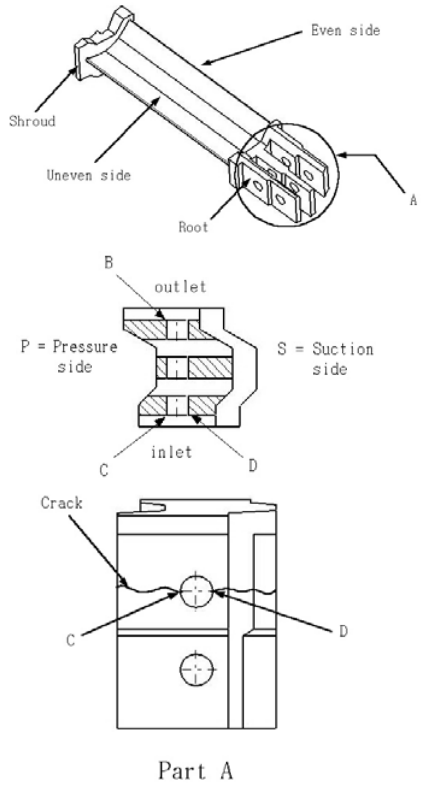

Fig. 1. Crack initiation and growth position at third stage of LP turbine.

Fig. 1 shows the crack and its growth location around the front blade root. The crack starts from Point C or D around the upper pin hole, where stress is concentrated, and grows along the circumference of rotor parallel to the lone extended from CD. The phenomenon has frequently occurred in the blades provided by GE (General Electronics), whose appearance is similar to the illustration [5].

3. Material and experimental procedure

3.1 Materials and test specimen

The material used in the test was 12% Cr steel, which is used for the axial flow impulse low-pressure turbine in an atomic power plant.

Table 2 shows the chemical composition of 12% Cr steel and Table 3 shows the results of the tensile test of 12% Cr steel in the controlled setting of 252℃ and 33.3℃, the entry and exit temperatures of the low pressure turbine, respectively.

Fig. 2 shows the geometry and dimensions of the fatigue test specimen, which was collected and manufactured from a sound part of a destructed low pressure turbine blade [6].

Table 2. Chemical composition of 12% Cr steel (wt.%)

C	Si	Mn	Ni	Cr	Mo	V	P	S
0.21	0.50	0.55	0.55	12.0	1.0	0.3	0.025	0.02

Table 3. Mechanical properties of 12% Cr steel

Temp. (℃)	Yield strength σ_{ys}(MPa)	Tensile strength σ_{ts}(MPa)	Poisson ratio ν	Elongation ε_f(%)	Young's modulus E(GPa)
20	670	790	0.29	26.4	203
252	596	745	0.288	10.8	202

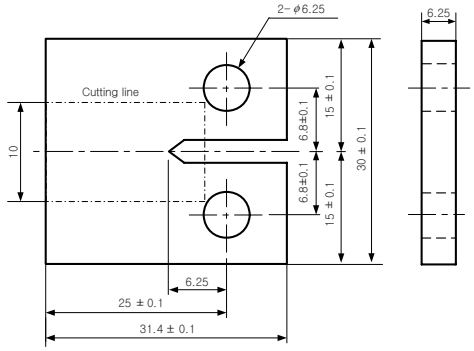

Fig. 2. Geometry and dimension of CT specimen.

3.2 Fatigue test

All of the tests on fatigue growth rate were conducted with a 49kN fatigue testing system occupying the closed-loop servo-hydraulic units (SHIMADZU EIIF-EB5-10L) [7], following the procedure described in the ASTM E 647 standard, the general fatigue crack growth test method which evaluates the stress ratio with the load range set in a fixed state for every test condition [6]. However, the study had to execute failure analysis, so it was very important to calculate the mean stress applied to the turbine blade and the stress amplitude. The mean stress that occurs in the pin hole of a turbine blade is induced by the centrifugal force of the rotation rate of the rotor and the torsion displacement by the torsion mount and it was 3.8MPa by the finite element analysis [8]. Therefore, assuming that the minimum engineering stress was 3.8MPa, the fatigue test was executed in 4 levels of partly pulsating load range where the minimum engineering stress was 3.8MPa : 1.5kN, 4.7kN, 7.6kN and 22.7kN. The stress intensity factor, K, was determined by the crack length, a, and the applied load, P, as represented in Eq. (1). The crack growth length was measured with the help of a low power traveling microscope.

$$K = \frac{P}{B\sqrt{W}} \frac{(2+a)}{(1-a)^{3/2}} (0.886 + 4.64(a/W) - 13.32(a/W)^2 + 14.72(a/W)^3 - 5.6(a/W)^4) \quad (1)$$

Where, a is the crack length, and W and B represent the width and thickness of the used specimen, respectively.

3.3 Atomic force microscope

Fig. 3 shows the appearance and measurement principle of the atomic force microscope. In short, the cantilever bends up or down due to the force generated between the probe on the tip of the cantilever type small rod and the atom on the surface of material depending on the shape of the material's surface, and at the moment, the flexural strength level on the material surface can be estimated by measuring the angle at which laser beam is reflected on the top of the cantilever.

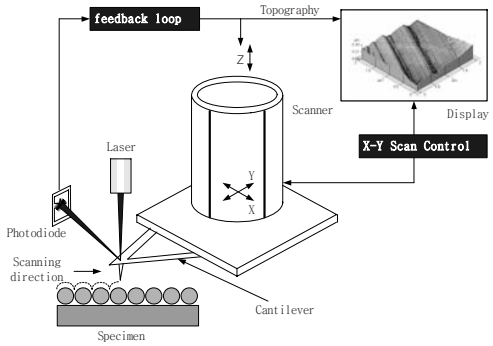

Fig. 3. Schematic diagram of atomic force microscope.

3.4 Failure analysis test

To execute the fracture surface of the turbine blade fractured by fatigue, a scanning electronic microscope (JEOL : JSM-35CF) was primarily used up to X1000. In addition, an atomic force microscope (PSIA model : AutoProbe CP Research) was used to examine the fatigue fracture surface in the nano scale area. By repeat measurements of the striation along the crack growth direction and the specimen thickness direction, the correlation between the striation interval in the 3-D image and the range of the stress intensity factor was reviewed. Then, the correlation with the fracture mechanical parameter was considered by measuring the surface roughness in the scan volume by an atomic force microscope at a precision of 0.1 nm. Fig. 4 shows the calculation method of Rq, the root mean square roughness on the roughness curve observed by an atomic force microscope [9].

4. Results and disscusion

4.1 Characteristics of fatigue crack growth

Fig. 5 shows the correlation between the fatigue crack growth rate of 12% Cr steel and the rate of the

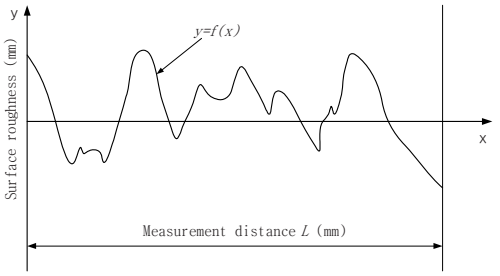

$$R_q = \sqrt{\frac{1}{l}\int_0^l f(x)^2\,dx}$$

Fig. 4. Schematic representation of various surface roughness parameters for fracture surface.

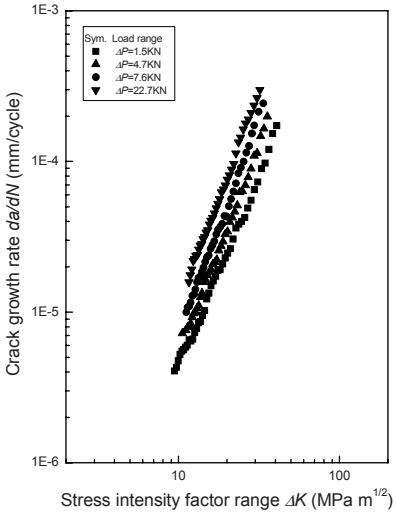

Fig. 5. Relation between stress intensity factor range and crack growth rate.

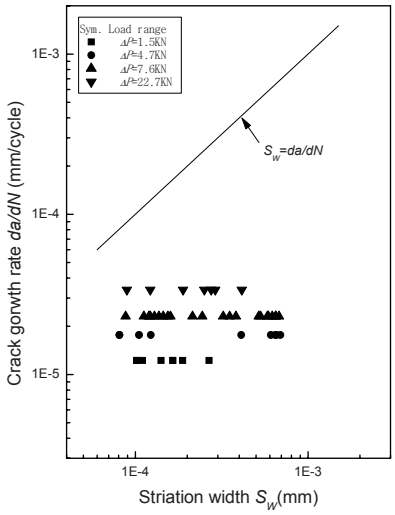

Fig. 7. Relation between 3-dimensional striation width and crack growth rate at $\Delta K = 15MPa\sqrt{m}$.

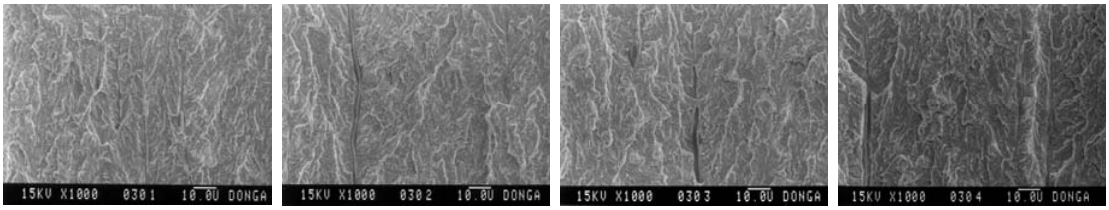

(a) $\Delta K = 10MPa\sqrt{m}$ (b) $\Delta K = 15MPa\sqrt{m}$ (c) $\Delta K = 20MPa\sqrt{m}$ (d) $\Delta K = 25MPa\sqrt{m}$

Fig. 6. SEM fractography for 12% Cr steel at $\Delta P = 7.6kN$.

stress intensity factor. When the crack growth rate increased with the increase of the load range for the same stress intensity factor, the material was considerably affected by the load range. Fig. 6 shows the fatigue fracture surface within the range of each stress intensity factor for 7.6kN of the same load range by using a scanning probe microscope. A typical ductile striation is not shown in the figure; instead, a small crack is repetitively formed in the direction of depth of fracture appearance perpendicular to the crack growth direction.

Fig. 7 shows the correlation between the range of the stress intensity factor and the intervals of small cracks for each load range, and the correlation with crack growth rate as a symbol and solid line, respectively. The intervals of small cracks to the same range of stress intensity factor show a difference from $\times 133$ up to $\times 16666$ compared with the crack growth rate, so it was found that small cracks were intermittently formed along the crack growth. Therefore, it seems that it is not reasonable to perform fracture surface analysis by using the interval of small cracks.

Fig. 8 shows each fracture area with origin at the pin hole of the fatigue fractured turbine blade observed by a scanning electronic microscope. As presented in Fig. 6, the distribution of small cracks looks irregular and the shape is not definite. Therefore, the failure analysis for the low pressure turbine blade may not be achieved by using a scanning electronic microscope used in the study. Fig. 9 shows the fracture surface for the same load range as observed by an atomic force microscope. A clear striation could be observed by the atomic force microscope, although it was in the area that could not provide the data useful for fracture surface analysis with the use of a scanning electronic microscope. A minute striation was observed in the area of a plateau by a scanning microscope. Therefore, even in the case of a brittle material whose striation is rarely found, a local striation that

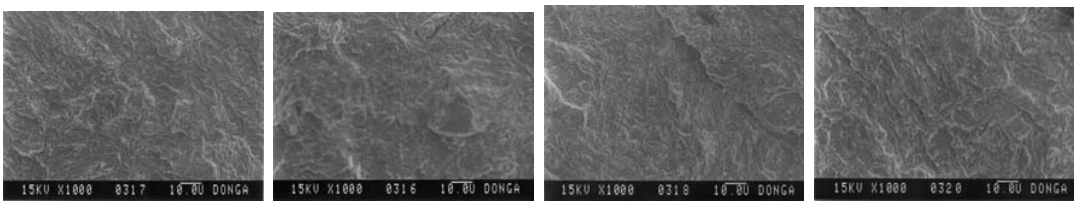

(a) a = 10.5 ㎜ (b) a = 18.5 ㎜ (c) a = 24.5 ㎜ (d) a = 30.5 ㎜

Fig. 8. SEM fractography for fatigue fractured turbine blade (a : distance from fractured turbine blade).

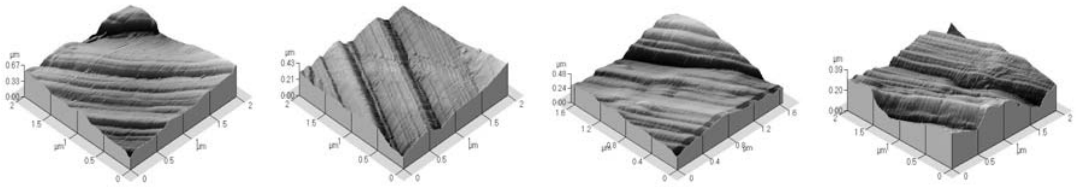

(a) $\Delta K = 10MPa\sqrt{m}$ (b) $\Delta K = 15MPa\sqrt{m}$ (c) $\Delta K = 20MPa\sqrt{m}$ (d) $\Delta K = 25MPa\sqrt{m}$

Fig. 9. AFM fractography for fatigue fracture surface at $\Delta P = 7.6kN$.

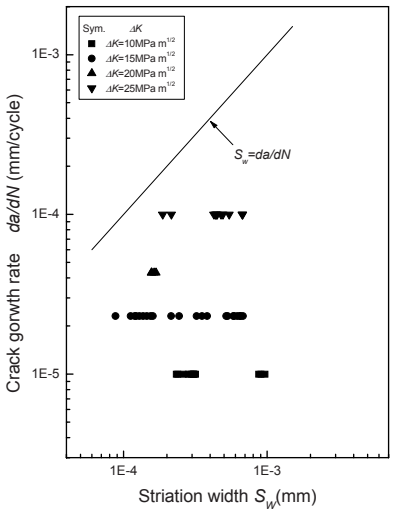

Fig. 10. Relation between 3-dimensional striation width and crack growth rate at $\Delta P = 7.6kN$.

was formed was observed by an atomic force microscope. However, the cross-sectional characteristics of the striation observed by the atomic force microscope did not rely on the load range.

Fig. 10 shows the interval of striation observed by an atomic force microscope and the crack growth rate, in the range of the stress intensity factor. The interval of striation was quietly distributed, irrespective of the range of the stress intensity factory and the load range. Such results might be interpreted as suggesting that ductile striation randomly relies on the crystal direction, while brittle striation is more sensitive to the load direction than the crystal direction. Thus striation was formed toward the crack growth direction, but the number was so small and the distribution was irregular. In addition, the interval of striation was as small as one-tenth the crack growth rate. Therefore, the scale of the load applied to a low pressure turbine blade cannot be estimated by the interval of striation measured by an atomic force microscope. To solve the above-stated problem, Fig. 11, which shows the surface roughness calculated, was used. It was assumed that the surface roughness curve gained by observing 250 areas toward the crack growth direction for each range of the stress intensity factor, 10, 15, 20, 25 $MPa\sqrt{m}$, by the atomic force microscope would be a roughness curve. In the figure, a solid line shows the data of the root mean square roughness, *Rq* for the length from the pin hole regressed by the method of least squares, while the dotted line shows the distribution of the root mean square roughness calculated from a CT test specimen under fatigue.

The distribution of the root mean square roughness calculated from the failure of the turbine blade exists in the range of the root mean square roughness calculated by the fatigue test of the CT test specimen. Fig. 11 shows that the slope of the root mean square roughness curve for the range of the stress intensity factor is almost uniform, regardless of the load range, while the root mean square roughness curve for the range of the stress intensity factor moves positively in

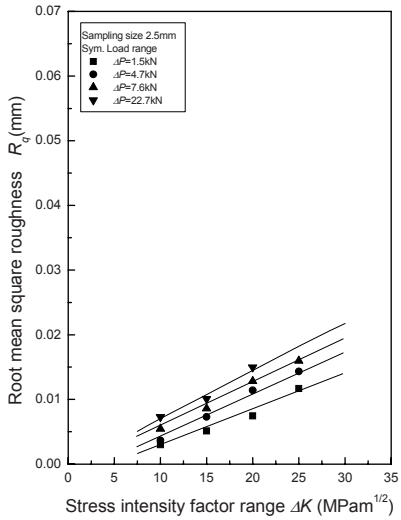

Fig. 11. Relation between ΔK and R_q in 12% Cr steel.

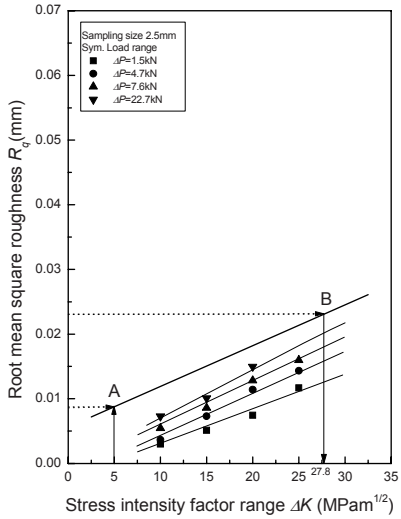

Fig. 12. Relation between R_q and gradient of R_q to ΔK.

parallel to the axis of root mean square roughness as the load range increases.

Therefore, the characteristic that fatigue crack growth will start when a load over the stress intensity factor range, ΔK_{th}, is applied to the material should be used to estimate the load of the turbine blade.

Considering that the range of the threshold stress intensity factor of stainless steel is 4.1-6.0 $MPa\sqrt{m}$ [10], it is assumed that the range of the threshold stress intensity factor of a turbine blade would be 5.0 $MPa\sqrt{m}$, the mean value. Fig. 12 shows the root mean square roughness for the stress intensity factor

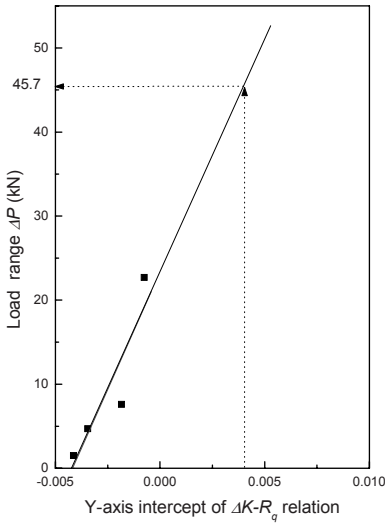

Fig. 13. Prediction of in-service load range using y-axis intercept of ΔK - R_q relation.

range for each load range, in which the dotted line shows the distribution of the root mean square roughness for the pin hole of the failure turbine blade. Point A is the cross point of one point where the stress intensity factor is 5.0 $MPa\sqrt{m}$ and the root mean square roughness from the start point of a pin hole of failure turbine blade, and Point A is the start point of the fatigue crack growth. From the above, it could be found that after drawing the average slope of the root mean square roughness for the stress intensity factor range calculated in each fatigue test at Point A, the point where the last point of the failure turbine blade's pin hole meets the root mean square roughness is Point B; so the maximum stress intensity factor range applied to turbine blade's pin hole would be 27.8 $MPa\sqrt{m}$.

Fig. 13 shows the axis intercept of the root mean square in Fig. 12 for each load range and the linear regression equation can be expressed as follows:

$$\Delta P = 5589 \times R_q + 23.3 \quad (2)$$

Therefore, the load range applied to the turbine blade can be calculated as 45.7kN by substituting the vertical axis intercept of the root mean square roughness curve for turbine blade in Fig. 11, 0.004, to Eq. (2).

5. Conclusions

The study estimated the load conditions applied to

a turbine blade from the correlation between the stress intensity factor range and the root mean square roughness observed by an atomic force microscope through a fatigue crack growth test of 12% Cr steel, which is used for low pressure turbine blades, to investigate the causes of failure in a torsion-mounted type turbine blade used for a low pressure turbine in an atomic power plant.

(1) A minute striation by cyclic slip band might be observed by using an atomic force microscope, although brittle striation was hardly observed by a scanning probe microscope.

(2) A linear correlation did not exist between the interval of brittle striation estimated by an atomic force microscope and the stress intensity factor range.

(3) The load condition of failure turbine blade could be estimated because the root mean square roughness measured by an atomic force microscope had a clear linear correlation with the stress intensity factor range.

Acknowledgement

This Paper was supported by Dong-A University Research Fund.

References

[1] H. J. Park, Introduction to Steam Turbine Blade, *J. of the KSME*, 38 (8) (1998) 44-49.

[2] H. C. Teichman, Analytical and experimental simulation of fan blade behavior and damage under bird impact, *Journal of engineering for gas turbines and power*, 113 (1991) 582-594.

[3] S. I. Park, J. W. Hong and Y. G. Noh, Scanning probe microscopy, PSIA, (2000) 3-15.

[4] H. Masude, N. Nagashima and S. Matsuoka, In-situ observation on metal surface in aqueous solutions with electrochemical STM, *J. of JSME*, 57 (1991) 2270-2277.

[5] Korea Plant Service & Engineering, 3ed Seminar on the Turbine Technology, KPS Co. Ltd., (1999) 141-162.

[6] ASTM Standard E647-93, Standard test method for measurement of fatigue crack growth rates, *ASTM standards Sec. 3*, 03.01 (1994) 591-596.

[7] Shimadzu, EHF-EB5-10L Type User's Manual, Shimadzu Co., (1993) 54-55.

[8] Hong S. H., Cho S. S., Joo W. S., A Study on the Safety Estimation of Low Pressure Torsion mounted Turbine Blade, *J. of KSPE*, 20 (3) (2003) 149-156.

[9] J. H. Park, Precise Measurement Engineering, Ya-Jeong Publishers, (1996) 257-286.

[10] H. O. Fuchs and R. I. Stephens, Metal fatigue in engineering, Willy-inter science publication, (1980) 301.